ChemPubSoc Europe

DOI: 10.1002/chem.201903439

CHEMISTRY A European Journal Full Paper

Main-Group Chemistry

Understanding the Localization of Berylliosis: Interaction of Be^{2+} with Carbohydrates and Related Biomimetic Ligands

Matthias Müller and Magnus R. Buchner*[a]

Abstract: The interplay of metal ions with polysaccharides is important for the immune recognition in the lung. Due to the localization of beryllium associated diseases to the lung, it is likely that beryllium carbohydrate complexes play a vital role for the development of berylliosis. Herein, we present a detailed study on the interaction of Be^{2+} ions with fructose and glucose as well as simpler biomimetic ligands, which emulate binding motives of saccharides. Through NMR and IR spectroscopy as well as single-crystal X-ray diffraction, complemented by competition reactions we were able to determine a distinctive trend in the binding affinity of these ligands. This suggests that under physiological conditions beryllium ions are only bound irreversibly in glycoproteins or polysaccharides if a quasi ideal tetrahedral environment and κ^4-coordination is provided by the respective biomolecule. Furthermore, Lewis acid induced conversions of the ligands and an extreme increase in the Brønstedt acidity of the present OH-groups imply that upon enclosure of Be^{2+}, alterations may be induced by the metal ion in glycoproteins or polysaccharides. In addition the frequent formation of Be-O-heterocycles indicates that multinuclear beryllium compounds might be the actual trigger of berylliosis. This investigation on beryllium coordination chemistry was supplemented by binding studies of selected biomimetic ligands with Al^{3+}, Zn^{2+}, Mg^{2+}, and Li^{+}, which revealed that none of these beryllium related ions was tetrahedrally coordinated under the give conditions. Therefore, studies on the metabolization of beryllium compounds cannot be performed with other hard cations as a substitute for the hazardous Be^{2+}.

Introduction

Metal-induced immune reactions play an important role in the body's defense against pathogens. For example aluminium compounds are added to vaccinations to increase their efficiency.[1,2] Though, there is still little known on the mechanism of action.[3–5] Only in the last decade it was discovered that the aluminium ion directly interacts with the major histocompatibility complex II (MHCII) on the surface of dendritic cells, which present antigens to T-cells.[6,7] This receptor arbitrarily binds proteins within the body and then binds to the T-cell receptor. If a foreign protein is bound, an immune response is triggered. Current research indicates that beryllium ions, which exhibit the same charge to ion radius ratio as Al^{3+}, also show a high affinity to the MHCII. The incorporation of Be^{2+} into a self-peptide bound to the MHCII leads to the recognition of this peptide as a threat by T-cells.[8–10] However, it is still unknown how and where the beryllium ions actually bind.

The MHCII is present on the surface of all antigen presenting cells throughout the body, since it is one of the fundamental immune recognition mechanisms. Indeed, beryllium associated diseases are known to be extremely lung specific. The so-called berylliosis causes the formation of granulomata, which are related to the beryllium-affected areas of the lung tissue.[11–14] While recent research indicates that the formation of these granulomata is related to hypersensitized T-cells that bind to the MHCII of antigen presenting cells,[9,10] this does not explain the localization to the lung. Yet, the immune recognition in the lung is also strongly dependent on the interaction of polysaccharides on the surface of pathogens with proteins in the lung.[15] These polysaccharides build up the outer layer of the cell membrane, the so-called glycocalyx. This pericellular matrix encapsulates also body-own cells and plays a major role for the correct interaction between T-cells and the MHC-receptors.[16,17] Furthermore many processes related to the immune system—especially in the lung—are controlled by the interaction of glycanes with proteins, which are partly Ca^{2+} dependent.[15,17–20] However, much is still unknown about the interaction of glycans, their co-factors, and the proteins of the immune system. Due to the high oxophilicity of beryllium ions it is likely that these bind strongly to polysaccharides and interfere with the protein—carbohydrate interaction or replace Ca^{2+} as a co-factor and thereby trigger an autoimmune reac-

[a] M. Sc. M. Müller, Dr. M. R. Buchner
Anorganische Chemie, Nachwuchsgruppe Berylliumchemie
Fachbereich Chemie, Philipps-Universität Marburg
Hans-Meerwein-Straße 4, 35032 Marburg (Germany)
E-mail: magnus.buchner@chemie.uni-marburg.de
Homepage: http://www.uni-marburg.de/fb15/ag-buchner

Supporting information and the ORCID identification number(s) for the author(s) of this article can be found under: https://doi.org/10.1002/chem.201903439.

tion.[21] Thus, knowledge about the reactivity of beryllium compounds towards carbohydrates could provide data to evaluate the impact of beryllium on glycoproteins that are related to the MHCII and give valuable insights as to why beryllium associated diseases are selectively localized to the lung.

To the best of our knowledge there are no comprehensive studies about the interactions of beryllium and carbohydrates nor on appropriate model systems. As a strong Lewis acid, Be^{2+} should show partly comparable reactivities to related hard cations, like Al^{3+} or Cr^{3+} and in contrast to Be, numerous studies have been published on the reactivity of these[22–26] and other Lewis acids[27–30] towards saccharides. As a consequence we decided to contribute to this field and study the reactivity of beryllium ions on carbohydrates and suitable model systems.

To understand the reactivity of sugars with Be^{2+} cations and to predict the coordination of Be^{2+} cations inside oligo- and polysaccharides in vivo we performed experiments on glucose and fructose as wells as on simpler model systems that mimic the coordination sites of these two common carbohydrates. A summary of the employed model ligands and their relation to the sugars is given in Figure 1. Furthermore, we reacted $BeCl_2$-related (pseudo) main-group metal chlorides (Li^+, Mg^{2+}, Al^{3+} and Zn^{2+}) with selected model ligands for comparison. This revealed relations but also significant differences between some of the tested metal ions and answers the long standing question if it is possible to emulate the coordination environment at the beryllium cation around other metal ions. Because if Be^{2+} was substitutable by other metal cations, researchers on the field of berylliosis could access a larger data base to evaluate the most likely binding sites for beryllium inside affected proteins under much safer conditions.

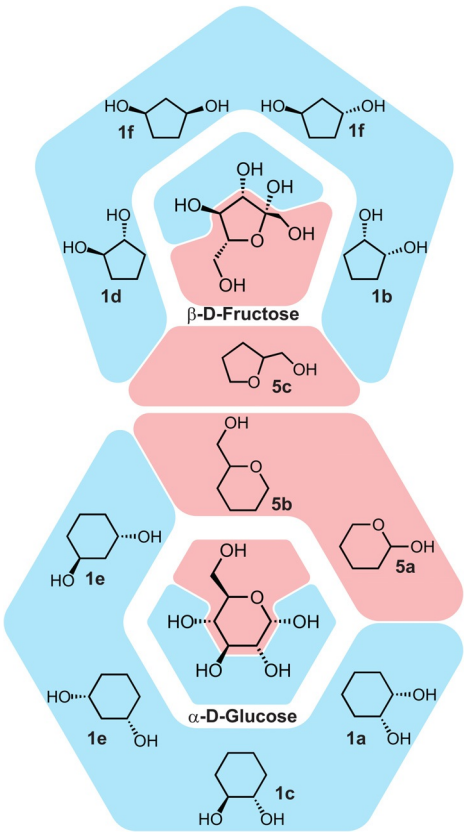

Figure 1. Illustration of the used ligands to mimic the coordination sites of glucose and fructose.

Beryllium compounds with cyclic diols

There are two mayor problems with the use of sugars as ligands in beryllium coordination chemistry. On the one hand they are insoluble in non-coordinating solvents, whereas the use of appropriate coordinating solvents, like water or methanol, leads to competition for coordination to the beryllium atom between solvent and ligands. Due to the lack of basic knowledge of the solution chemistry of beryllium compounds,[31] the resulting dissociation equilibria are hence too complicated for immediate interpretation. On the other hand, sugars offer various coordination sites and their NMR spectra show complex signal sets even without coordination towards a metal cation. Thus a principle understanding of the coordination behavior of simpler ligands towards Be^{2+} had to be gained first. For this reason preceding investigations with cyclohexanediols and cyclopentanediols were conducted. Therefore, $BeCl_2$ was reacted with these simple cyclic diols in a 1:1 and a 1:2 ratio in $CDCl_3$.

While *cis*-1,2-cyclohexanediol (**1a**), *cis*-1,2-cyclopentanediol (**1b**), *trans*-1,2-cyclohexanediol (**1c**), and *trans*-1,2-cyclopentanediol (**1d**) were used in their isomerically pure form, 1,3-cyclohexanediol (**1e**) and 1,3-cyclopentanediol (**1f**) were only available as a *cis*/*trans* mixture and had to be used without prior purification. When $BeCl_2$ was reacted with one equivalent of diols **1** in $CDCl_3$ in J. Young NMR tubes, we observed precipitation of colorless to yellow solids as shown in Figure S1, Supporting Information. The amount as well as the consistency of these precipitates already pointed towards differences between the used diols. The highest amount of solid residue was obtained when *cis*-1,2-diols **1a** and **1b** were used, whereas *trans*-1,2-diols **1c** and **1d** showed the least amount of precipitate. The reaction between $BeCl_2$ and 1,3-diols **1e** and **1f**, respectively, resulted in a more dense and mucilaginous precipitate. Due to the considerable amount of precipitate the recorded NMR spectra showed a strong line broadening and partly no signals, which made a systematic evaluation of the obtained spectra impossible. In addition, the signals become more complex due to the coordination towards beryllium, because the mobility of the hexyl and pentyl rings, respectively is limited by the metal coordination and the protons become distereotopic. We, therefore, only discuss the chemical shifts of the *CH*OH- and the *HO*-protons, which show the most distinct coordination shift. For the C*H*OH nuclei we observed a downfield shift of $\Delta\delta = 0.59$ and 0.57 ppm for *trans*-1,2-diols **1c** and **1d**, respectively, compared to the free diols, while the corresponding protons of *cis*-1,2-diols **1a** and **1b** are shifted downfield by $\Delta\delta = 0.38$ and 0.10 ppm, respectively. On the other hand, 1,3-diols **1e** and **1f** show no coordination shift. However, the signal intensities for the *cis* standing 1,3-diols lowered significantly, leading to the assumption that *cis*-1,3-cyclohex-

anediol and *cis*-1,3-cyclopentanediol, respectively, precipitated while their corresponding *trans* standing diols stayed in solution. The same observation was made for the proton of the OH groups of the 1,3-diols. The respective *OH* NMR signals of the 1,2-diols **1a**–**d** show the same trend observed for their *CH*OH protons. While **1c** and **1 d** show a downfield shift of $\Delta\delta = 6.04$ and 6.20 ppm, the OH group of **1a** is shifted by $\Delta\delta = 4.98$ ppm and **1b** only by $\Delta\delta = 0.83$ ppm (see also Figures S12–S17, Supporting Information). In addition, we did not observe any signal in the ^{9}Be NMR spectra of the 1:1 reaction mixtures in $CDCl_3$, which indicates that most of the formed beryllium compounds did precipitate and the signals of the beryllium nuclei that remained in solution undergo severe line broadening. When these solutions were stored for several weeks the precipitate of the **1b** containing NMR tube recrystallized to yield colorless rod-shaped crystals of tetra(κ^2-*cis*-cyclopentane-1-μ_2-olate-2-ol beryllium) tetrachloride (**2a**), the molecular structure of which is illustrated in Figure 2.

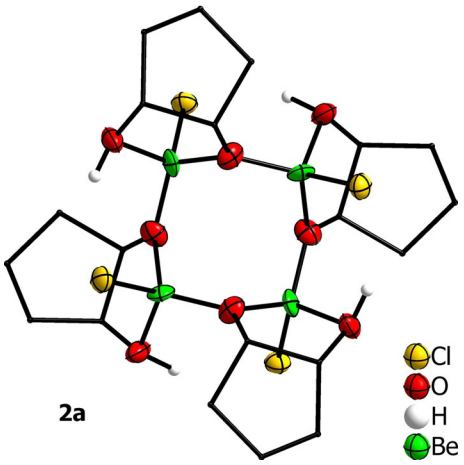

Figure 2. Molecular structure of complex **2a**. Ellipsoids are depicted at 70% probability at 100 K. Carbon-bound hydrogen atoms are omitted and carbon atoms are shown as wire frame for clarity.

We assume slow evolution of HCl occurs during the recrystallisation of the initial precipitate. Compound **2a** features a heavily tilted eightfold Be–O ring that is built up of four $[BeCl]^+$ units each of which is coordinated by a single deprotonated *cis*-1,2-cyclopentanediol. These subunits are μ_2-bridged by the olate groups of the four mono-deprotonated *cis*-1,2-cyclopentanediol ligands. The Be–Cl atomic distances are 2.016(11) and 2.028(11) Å, which is longer than those reported for μ_2-bridged olato complexes tetrakis(μ_2-*t*-butoxy)-dichloro-tri-beryllium[32] with 1.866(3) and 1.886(3) Å and a beryllium calixarene complex[33] with 1.943(3) and 1.946(3) Å. The Be–O atomic distances within the eightfold Be–O ring range from 1.589(12) to 1.610(12) Å and are, therefore, longer than the corresponding distances in the *t*-butoxy beryllium compound[32] mentioned above but shorter than those reported for the calixarene complex[33] and a fully deprotonated diol complex reported by Klüfers[34] with Be–O atomic distances of 1.624(2) to 1.648(2) Å. The exocyclic Be–O atomic distances towards the hydroxy groups are 1.703(12) and 1.716(13) Å, which is longer compared to 1.6268(12) Å reported for the benzyl alcohol adduct towards $BeCl_2$.[35] These longer distances suggest rather high electron density at the beryllium atom. The IR spectrum of **2a** reveals a bathochromic shift for the O–H stretching frequency of 159 cm^{-1} and a significantly reduced band width compared to the free diol **1b** indicating a small weakening of the O–H bond.

When $BeCl_2$ was reacted with two equivalents of the respective diols **1** under identical conditions, we obtained similar amounts of precipitate compared to the 1:1 reactions, which were in case of **1a**, **1b**, and **1e** micro-crystalline. The NMR studies on these reaction mixtures follow the trend of the previous reactions but with increased line broadening and signal intensity. This suggests higher solubility of the formed compounds and exchange on the NMR timescale between species in solution and the solid. Additionally, a slight increase in the downfield shift of around $\Delta\delta = 0.1$ ppm for the *CH*OH groups compared to the 1:1 reactions (see also the Supporting Information, Table S4) was observed. For **1a** we find a broad signal for the OH group at $\delta = 8.05$ ppm, which is a significant increase compared to $\delta = 7.17$ ppm observed in the 1:1 reaction, whereas the other 1,2-diols did not show a significant OH signal in the ^{1}H NMR spectra. The latter is indicative for a severe weakening of the O–H bond strength, which leads to partial proton dissociation in solution. In the ^{13}C NMR spectra an increase of the line broadening compared to the 1:1 reactions was observed, which is in line with the broader signals in the ^{1}H NMR spectra. Furthermore no signals were observed in the ^{9}Be NMR spectra. To overcome the solubility problems in non-coordinating solvents we moved to liquid SO_2 as weakly coordinating solvent. Sulfur dioxide has the advantage that it can coordinate towards anions via its sulfur atom, while the oxygen atoms are relatively bad ligating sites. Thus, we reacted diols **1** with $BeCl_2$ in a 2:1 ratio and initially received clear colorless solutions, from which colorless single crystals in nearly quantitative amounts were obtained within minutes in case of diols **1a**,**b**,**e**. The ^{1}H NMR spectra recorded directly after the starting materials had dissolved show several multiplets with immense line broadening and hydroxy protons that are shifted beyond $\delta = 10$ ppm and the ^{13}C NMR spectra show several discrete species. We also observed singlets in the ^{9}Be NMR spectra between $\delta = 2$ and 4 ppm that show medium line broadening in case of the 1,2-diols **1a**–**d**, whereas 1,3-diols **1e** and **1f** yielded narrow singlets. This chemical shift is in the typical region of fourfold coordinated beryllium nuclei.[36] The reduced line width of the **1e** or **1f** containing solutions compared to those containing **1a**–**d** indicates less exchange between the ligands and, therefore, a more stable species. According to the chemical shifts and line shape of the singlets, we assume that Be^{2+} cations are present in solution, which are tetrahedrally coordinated by diols **1**, as expected.

After the NMR spectra were measured the solvent was removed in vacuo. To do this, the tubes had to be cooled, which led to the bursting of the crystals. The IR spectra of the dry residues did show bathochromic shifts for the O–H stretching frequencies of around 700 to 900 cm^{-1} and increased band

broadening, which is considerably larger than in compound **2a**. The large bathochromic shifts indicate a significant weakening of the O–H bond due to the coordination towards Be^{2+} and that all investigated diols are equally affected. These observations coincide with those from ^{1}H NMR spectroscopy regarding the hydroxy protons.

Since the single-crystals obtained by the use of **1a**,**b**,**e** burst when the SO_2 was cooled or the pressure was released, we altered the reaction conditions. Substitution of $BeCl_2$ through $BeBr_2$ led to the same amount of single crystals within hours that now resisted the necessary temperature change to −78 °C during preparation for the X-ray structure analysis. For **1a** we obtained bis(κ^2-*cis*-1,2-cyclohexanediol)beryllium(II) bromide·2 SO_2 (**3a**) which crystallizes in the orthorhombic space group *P*bam. Compound **3a** features a $[Be(\mathbf{1a})_2]^{2+}$ cation (**4a**) that is surrounded by four bromide anions that are interacting through hydrogen bonds with the hydroxy groups. While no hydrogen bonds are formed to the surrounding solvate SO_2 molecules, the sulphur atoms of which show interactions to nearby bromide anions to form one-dimensional Br–SO_2 chains with Br–S atomic distances of 3.217(1) and 3.219(1) Å. These are larger than comparable Br–SO_2 distances in $NEt_4Br{\cdot}SO_2$[37] (3.0942(6) and 3.1161(7) Å) or $[N(CH_3)_3(C_{16}H_{33})]Br{\cdot}SO_2$[38] (2.992(5) Å). Cation **4a**, which is illustrated in Figure 3, shows disordered diol ligands in which the hydroxy groups change from axial to equatorial conformation in the cyclohexane and vice versa similar to a puckering hexose.

The Be^{2+} is coordinated tetrahedrally by four hydroxy groups with Be–O atomic distances of 1.562(3) Å (eq. OH group) and 1.693(3) Å (ax. OH group). This significant variance in bond length is also observed in κ^2-inositol complexes of Pr and Nd for which the axial hydroxy groups also tend to have a larger distance to the metal center compared to the equatorial hydroxy group. An inverse trend is reported for κ^3-1,2,3-cyclohexanetriol complexes instead.[39] The Be–$O_{ax.}$ atomic distance in **4a** is slightly larger but comparable with those of the deprotonated hydroxy group of **2a** or anionic complexes $Na_2[Be(O_3C_5H_6)_2]$[34] (1.6235(23) to 1.6477(22) Å) and $Na_2[Be(O_2C_6H_4)_2]$[40] (1.6317(62) to 1.6492(59) Å), while the Be–$O_{eq.}$ atomic distance in **4a** is significantly shorter. This indicates comparable ligating properties of neutral hydoxy and anionic olate oxygen atoms.

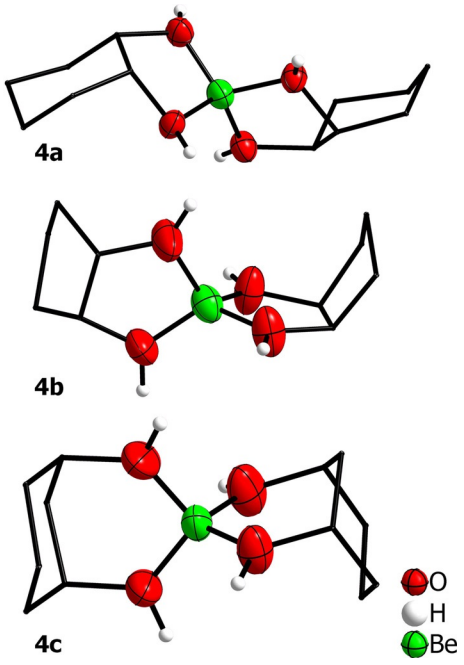

Figure 3. Molecular structures of complex cations **4a–c**. Ellipsoids are depicted at 70% probability at 100 K. Carbon-bound hydrogen atoms are omitted and carbon atoms are shown as wire frame for clarity. Subfigures are not to scale with each other.

In the case of diol **1b**, the formed crystals burst upon cooling. However, after the SO_2 was removed in vacuo the obtained microcrystalline powder could be recrystallized from CH_2Cl_2 to give crystals of bis(κ^2-*cis*-1,2-cyclopentanediol)beryllium(II) bromide·CH_2Cl_2 (**3b**) in the monoclinic space group $P2_1/c$. Compound **3b** features a $[Be(\mathbf{1b})_2]^{2+}$ cation (**4b**), which is depicted in Figure 3. It is surrounded by four bromide anions as in **4a**. The hydroxy groups of **4b** show Be–O atomic distances that range from 1.588(9) to 1.618(9) Å which is comparable to the Be–$O_{eq.}$ distance in **4a** but vastly shorter than those in **2a**. The short distances can be explained through the cationic nature of the complex ion. The resulting electron deficiency at the Be center needs to be compensated through stronger electron transfer from the *O*-ligands, which leads to contraction of the Be–O bond length.

The reaction of **1e** and $BeBr_2$ in SO_2 yielded single crystals of bis(κ^2-*cis*-1,3-cyclohexanediol)beryllium(II) bromide·3 SO_2 (**3c**) that crystallizes in the monoclinic space group $P2_12_12$. Compound **3c** features a $[Be(\mathbf{1e})_2]^{2+}$ cation (**4c**) similar to **4a** and **4b**. Compound **4c** is surrounded by four bromide anions like **4a**. The bromide anions form hydrogen bonds to two **4c** cations each and do not show a significant interaction towards the solvate SO_2 molecules. Compound **4c** does not show puckering like **4a** and its hydroxy groups are both in an axial conformation, which is illustrated in Figure 3. The Be–O atomic distances are with 1.596(10) and 1.627(11) Å shorter compared to the anionic complexes mentioned above and in between those of **4a** but show large standard deviations due to the low quality of the obtained data. The O-Be-O bite angle is 103.9(9)°, which is significantly larger than the corresponding angles of **4a** (95.5(2)°), **4b** (92.9(5)–94.6(5)°), and **2a** (95.3(6)–97.1(6)°). The less strained O-Be-O angle of **4c** gets in the range of the ideal tetrahedral angle and supports the better ligating properties of 1,3-diols compared to the 1,2-diols, which were also deducted from the NMR spectroscopic data. A plausible pathway for the formation of **2a** and **3b** is given in Scheme 1.

While we were able to obtain the crystalline compounds **3a–c** and **2a**, attempts to obtain crystal for Be complexes with *trans*-diols **1c,d** failed. We assume this is caused by the coordination geometry that is dictated by the hydroxy groups of the *trans*-diols. Since *trans*-diols tend to build up nontetrahedral coordination polyhedra around metal cations with reported bite angles of 79.6–81.7°,[41,42] which are unlikely to be realized around the small Be^{2+} cation, which is rarely found in nontetrahedral coordination environments. Accordingly, the resulting

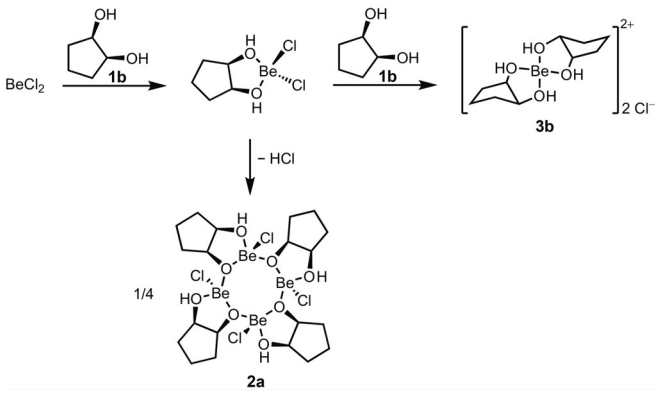

Scheme 1. Formation of **2a** and **3b** through reaction of $BeCl_2$ with one or two equivalents of **1b**.

precipitates of the *trans*-diols should be coordination polymers.

To determine which of the diols **1** binds best to beryllium we carried out competition reactions between the 1,2-diols. Therefore, we reacted $BeCl_2$ with two different 1,2-diols in a 1:2:2 ratio in $CDCl_3$ and obtained clear colorless solutions without any precipitate. The obtained ^{1}H NMR spectra revealed a clear trend in which the C*H*OH proton of the preferred diol was shifted between $\Delta\delta = 0.3$ and 0.5 ppm downfield while the corresponding proton of the competing diol was only shifted by about $\Delta\delta = 0.1$ ppm (see also the Supporting Information, Table S6). When two equivalents of *cis*-1,2-pentanediole (**1b**) compete with two equivalents *trans*-1,2-pentanediole (**1d**) or *cis*-1,2-hexanediole (**1a**), respectively, for $BeCl_2$, **1b** shows the highest coordination shift in the ^{1}H NMR spectra, indicating that it has a greater affinity for a coordination towards Be^{2+}. Accordingly, **1a** shows a higher tendency to coordinate towards $BeCl_2$ than *trans*-1,2-hexanediole (**1c**) when both are reacted in the same way.

Based on these results we can devise a clear trend for the beryllium binding capabilities of the different diol geometries. The least stable compounds are formed with the *trans*-1,3-diols. These show no coordination tendencies, which is presumably caused by the large distance between the OH-groups. Therefore, the small Be cation is not able to bind to both oxygen atoms of one ligand. The *trans*-1,2-diols are slightly better ligands and there is some indication that these can act as chelators for Be^{2+}. However the small bite angle results in coordination environments around the beryllium atom that differ significantly from the preferred tetrahedral one. Thus, the formed complexes exhibit vivid ligand dissociation processes in solution. *cis*-1,2-diols form stable complex cations with Be^{2+}, however, the bond angles around the Be atom are still below 100°. The competition reactions suggest that *cis*-1,2-cyclohexanediole (**1a**) is inferior to *cis*-1,2-cyclopentanediole (**1b**). This is presumably caused by the larger bite angle of the latter, which results in less ring strain when coordinated to beryllium. It is evident from the low solubility, the absence of ligand dissociation equilibria and the quasi tetrahedral bond angles around Be in complexes with *cis*-1,3-diols that this is the ligand geometry, which provides the most stable beryllium complexes. We deduct that sugars and polysaccharide with *cis* standing OH-groups in 1,3-position are the most likely binding sites for Be^{2+}.

Besides the relative binding affinity among the diols, the competitiveness of them against water is a key aspect to discuss. When the diols were added to an aqueous $BeCl_2$ solution, we only observed a singlet assigned to $[Be(H_2O)_4]^{2+}$ in the ^{9}Be NMR spectra and the ^{1}H and ^{13}C NMR spectra revealed that the diols are not affected by Be^{2+}. This leads to the conclusion that the diols are not capable to successfully compete with the large excess of H_2O ligands for beryllium coordination. Therefore, it is unlikely that hydrated beryllium cations are captured by carbohydrates under physiological conditions, if only two OH-groups of the carbohydrate are accessible for coordination.

Coordination of tetrahydropyranols and -furanols towards beryllium ions

Besides coordinating hydroxy groups that are bound to the pentyl and hexyl ring, respectively, carbohydrates feature a terminal CH_2OH group as well as an aldehyde/hemiacetal function. We have already reported on the reactions of beryllium halides with a variety of basic aldehydes, which led partly to polymerisation or degradation of the latter.[43] To transfer our results regarding these aldehydes towards carbohydrates, we reacted a simple hemiacetal with $BeCl_2$ and compared the results. If $BeCl_2$ is reacted 1:1 or 1:2 with tetrahydro-2*H*-pyran-2-ol (**5a**) in non-coordinating solvents, like chloroform, at ambient temperatures, $BeCl_2$ is not dissolved immediately. However, a colorless to yellowish suspension is obtained. Within two hours the suspension turns via brown to nearly black and an amorphous brown precipitate formed around the $BeCl_2$. NMR-monitored experiments revealed a fast degradation of **5a** into unknown polymeric species, which match our findings regarding simple aldehydes like isobutyraldehyde.[43] Because of the fast decomposition of **5a** we did not perform further experiments with similar hemiacetals. Instead we investigated the potential coordination of $BeCl_2$ by the terminal CH_2OH and the ether group. For this reason tetrahydro-2*H*-pyran-2-ylmethanol (**5b**) was reacted under the same conditions as **5a** with $BeCl_2$. The starting materials dissolved immediately and gave a clear colorless solution that remained stable for several weeks. The recorded NMR spectra (Figures S18 and S23, Supporting Information) show, in addition to the signals of **5b**, the appearance of a new signal set in case of the 1:1 reaction mixture and increased line broadening when a second equivalent **5b** is present in solution. The large amount of signals in the ^{13}C NMR spectra of the 1:1 reaction mixture indicates the presence of a variety of distinct species. In the 2:1 reaction mixture the signals in the ^{13}C NMR spectrum showed increased line broadening, which leads to the assumption that exchange on the NMR timescale takes place between the observed species. In the ^{9}Be NMR spectra the observed singlet at $\delta = 3.0$ ppm ($\omega_{1/2} =$ 31.2 Hz) speaks for a tetrahedrally coordinated species in the 1:1 reaction mixture. In the 2:1 mixture a second singlet emerged at $\delta = 4.1$ ppm ($\omega^{1/2} = 11.9$ Hz). The reduction of line width indicates a compound with higher symmetry in solution,

while the chemical shift range of both signals suggests fourfold coordination. The 1:1 $CDCl_3$ solution was diluted with pentane by gas-phase diffusion to obtain colorless needle-shaped crystals of tetra(κ^2-tetrahydro-2*H*-pyran-2-yl-μ_2-methanolate beryllium) tetrachloride (**2b**) that crystallizes in the tetragonal space group $P\bar{4}2_1c$. For the 2:1 solution, the same procedure yielded colorless oil droplets that separated from the solution. The molecular structure of **2b** in the solid state is illustrated in Figure 4.

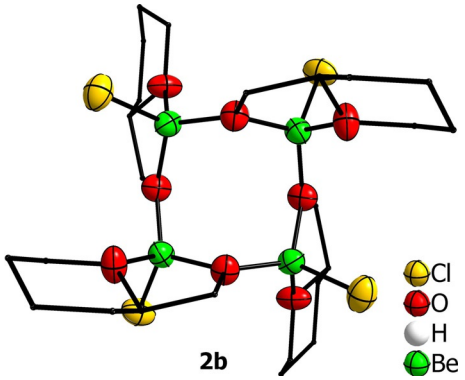

Figure 4. Molecular structure of complex **2b**. Ellipsoids are depicted at 50% probability at 100 K. Carbon-bound hydrogen atoms are omitted and carbon atoms are shown as wire frame for clarity.

Similar to compound **2a** an eight-membered Be–O ring is formed through the cleavage of HCl and the subsequent coordination of $BeCl^+$ by the deprotonated hydroxy group. The tetrahedral coordination sphere around the beryllium atom is completed by the ether oxygen atom instead of the additional hydroxy group in **2a**. Within the hexyl rings a disorder is present similar to those mentioned before. In direct comparison to compound **2a**, the Be–O atomic distances of the deprotonated hydroxy groups as well as the Be–Cl atomic distances and the O-Be-O bite angles are within the standard deviation identical (see Table 1). Also the Be–O atomic distance to the etheric oxygen atom (1.681(7) Å) equals that of the corresponding Be–O hydroxy distance in **2a**. Therefore, compound **2a** and **2b** are very similar to each other although their ligands are fundamentally different. Additionally, the structure of **2b** clearly revealed that, within the same ligand, hydroxy groups are superior binding sites for Be^{2+} compared to ether oxygen atoms. Due to the high solubility of the formed compounds we assume that noncharged compounds are present in solution. In accordance to the formation of compound **2a** and cations **4** we propose the complexation of $BeCl_2$ by **2b** takes place as depicted in Scheme 2. Initially one ligand coordinates to $BeCl_2$ under the formation of dichloro compound **6a**. This species slowly reacts under HCl evolution to the tetranuclear complex **2b**, while the presence of an additional equivalent of **5b** leads to the formation of neutral compound **7a**.

To translate the functionality of **5b** into a more fructose-like system we preformed analogous experiments with tetrahydrofuran-2-ylmethanol (**5c**). Here, we obtained a clear colorless solution when $BeCl_2$ and **5c** were reacted in $CDCl_3$. Whereas the

Table 1. Selected interatomic distances and angles of complexes **2a**,**b**, **4a**–**c**, **9b**,**c**, and **10a**–**d**.

	Be–OH [Å]	Be–O [Å]	Be–Cl [Å]	O-Be-O [°][a]
2a	1.703(12); 1.716(13)	1.589(12)-1.610(12)	2.016(11); 2.028(11)	95.3(6)–97.1(6)
2b	–	1.592(7); 1.620(7)	2.000(6)	95.1(3)
4a	1.562(3); 1.693(3)	–	–	95.5(2)
4b	1.588(9); 1.618(9)	–	–	92.9(5), 94.6(5)
4c	1.596(10)–1.627(11)	–	–	103.9(3)
9b	1.653(4)–1.672(4)	1.559(4)–1.605(4)	–	99.1(2)–107.8(2)
9c	1.679(3)–1.692(2)*c*	1.554(2)–1.633(2)	–	100.4(1)–107.6(1)
	M[b]–OH/Å	M[b]–O [Å]	M[b]–Cl [Å]	O-M[b]-O [°][a]
10a	1.946(3)–2.169(3)	–	–	77.9(1); 78.7(1)
10b	2.058(2)–2.117(2)	–	2.2548(6)–2.2989(6)	76.4(1)-77.8(1)
10c	2.029(8)–2.093(1)	–	–	76.1(1); 77.1(2)
10d	1.938(3)	1.835(3)	2.154(2); 2.156(2)	81.0(1)

[a] O-Be-O bite angles. [b] ^{9}Be related metals. [c] contacts to $[OH]^-$ excluded.

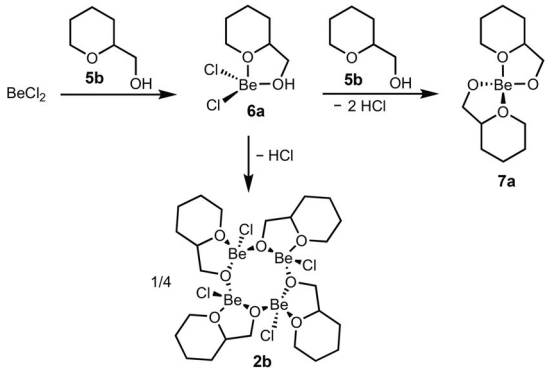

Scheme 2. Formation of **2b** and **7a** through reaction of $BeCl_2$ with one or two equivalents of **5b**, respectively.

^{9}Be NMR spectra are nearly identical to those recorded for **5b** and the ^{1}H and ^{13}C NMR spectra show the same behavior as described for **5b**, we were not able to obtain single crystals from the reaction solution. Every attempt to obtain the analogous compound to **2b**—tetra(κ^2-tetrahydrofuran-2-yl-μ_2-methanolate beryllium) tetrachloride (**2c**)—ended in the formation of a clear colorless oil, that did not dissolve in nonpolar solvents like benzene or pentane. The comparison of the IR spectra of the obtained oil of **2c** and the crystalline powder of **2b** reveals that the O–H stretching frequency of **2b** experiences a bathochromic shift of 794 cm^{-1} and shows immense line broadening. A similar shift of 810 cm^{-1} is also observed for supposed compound **2c** but with an additional more intense band that is only shifted by 186 cm^{-1} to lower wave numbers compared to **5c**. This might indicate that **5c** and **5b** form similar complexes with Be^{2+}.

To determine the relative binding affinities competition reactions were carried out between two equivalents of tetrahydro-

furan-2-ylmethanol (**5c**) and tetrahydro-2*H*-pyran-2-ylmethanol (**5b**) each in the presence of one equivalent $BeCl_2$. In the ^1H and ^{13}C NMR spectra broadening of the signals of both ligands was observed as well as coordination shifts. The broadening and shift change are similar for **5b** and **5c**, suggesting comparable binding properties towards Be^{2+}. This is not surprising since the bite angle, steric demand and electron density of both ligands is practically identical. Reactions of **5b** or **5c** with $BeCl_2$ and either *cis*-1,2-cyclohexanediol (**1a**) or *cis*-1,2-cyclopentanediol (**1b**) in a 2:1:2 ratio reveals that exclusively the signals of the diols are broadened and shifted. This proves that the *cis*-1,2-diols are superior ligands for Be^{2+}. Therefore, the coordination strength of these furanyl and pyranyl alcohols rank in between cyclic *cis*- and *trans*-1,2-diols. Hence it is very unlikely that beryllium ions bind to the oxygen atom of the glycosidic bond in polysaccharides, considering the abundance of OH groups available for coordination.

Beryllium compounds with *cis*,*cis*-1,3,5-cyclohexanetriol

Because bidentate diols proved to be insufficient chelators for Be^{2+} to compete with water, we tested a tridentate cyclic triol for a more advanced picture of a possible coordination towards carbohydrates. So we reacted *cis*,*cis*-1,3,5-cyclohexanetriol (**8**) with $BeCl_2$, to obtain information how κ^3-coordination towards beryllium can be achieved. The insolubility of **8** and $BeCl_2$ in the previously used solvents ($CDCl_3$, CD_2Cl_2 and SO_2) led to no reaction. Hence we had to resort to coordinating solvents, like methanol, DMF and water, with which we obtained colorless clear solutions. In the ^1H and ^{13}C NMR spectra of the aqueous and methanolic reaction solutions we did not observe any coordination shifts for the O*H* nor the C*H*OH protons and the ^9Be NMR spectra indicated tetrahedral coordination solely by solvent molecules around the beryllium nuclei. This is supported by the fact that when the solvents were removed in vacuo only free **8** recrystallized. However, the ^1H and ^{13}C NMR spectra of the DMF solutions revealed a coordination shift and broadening of the O*H* signal and the ^9Be NMR spectrum showed a signal at $\delta = 2.1$ ppm, which is different to the signal set observed for neat $BeCl_2$ dissolved in DMF. We, therefore, assume that dicationic species **9a** is formed (Scheme 3). Though we were not able to isolate this compound nor obtain single crystals.

Since deprotonation occurred with some of the above mentioned bidentate ligands, we tried to enforce this reactivity in **9a** by heating the reaction solution. However, even upon heating the reaction solution for several days at 180 °C, we did not observe a change in the NMR spectra. Only after the addition of beryllium metal and heating to 180 °C in a sealed tube we did observe the emergence of a new NMR signal set and after one hour a colorless precipitate was obtained. We attempted to measure the NMR spectra of this residue by redissolving it in SO_2. However, as soon as the precipitate came into contact with liquid SO_2, colorless single crystals grew on top of it. When the SO_2 was removed by opening the valve of the reaction vessel, the crystals remained stable and could be analyzed

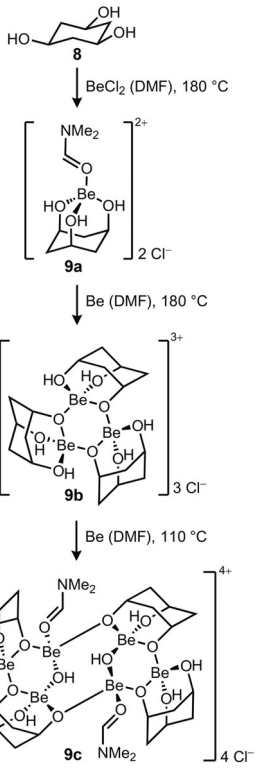

Scheme 3. Reaction of **8** with $BeCl_2$ and Be in DMF to yield **9b** and **9c**.

by X-ray diffraction. These crystals comprise of tris(κ^3-*cis*,*cis*-1,3-hydroxy-μ_2-5-olate-cyclohexane beryllium) trichloride·3 SO_2 (**9b**) and crystallize in the orthorhombic space group *Pbca*. The compound features a Be–O six-membered heterocycle with κ^3-coordinated Be^{2+} cations. All Be atoms in **9b** have the same coordination environment. Each Be atom is κ^3-coordinated by a single deprotonated **8** ligand, the μ_2-olate groups of which build up the heterocycle by completion of the tetrahedral coordination sphere of a neighboring Be atom. The resulting complex cation is illustrated in Figure 5.

Heating of **9b** in DMF at 110 °C for a prolonged time leads to the formation of colorless single crystals of bis(*N*,*N*-dimethylformamide-μ_2-hydroxido-κ^3-*cis*,*cis*-1,3-hydroxy-μ_2-5-olate-cyclohexane-κ^3-*cis*,*cis*-1-hydroxy-μ_2-3,5-di-olate-cyclohexane triberyllium) tetrachloride·3.5 DMF (**9c**) in the triclinic space group $P\bar{1}$ the molecular structure of which is shown in Figure 5. The unexpected structure of complex **9c** can be described as two Be–O six-membered rings, identical in their coordination, which are bridged by two olat groups from two different **8** ligands to form an eight-membered Be-O-heterocycle. A similar structural motive has already been observed for Be glycolate complexes.[44] Each of the beryllium atoms within the six-membered ring has a different coordination environment. The first of the Be atoms is κ^3-coordinated by a doubly deprotonated **8** ligand, the two deprotonated μ_2-olate groups of which coordinate towards two other Be atoms. The tetrahedral coordination sphere around the first Be atom is then completed by a μ_2-hydroxide anion that binds to the second Be atom, that is, κ^1-coordinated tetrahedrally by the doubly deprotonated **8** ligand of the second six-membered ring, an oxygen atom of a DMF

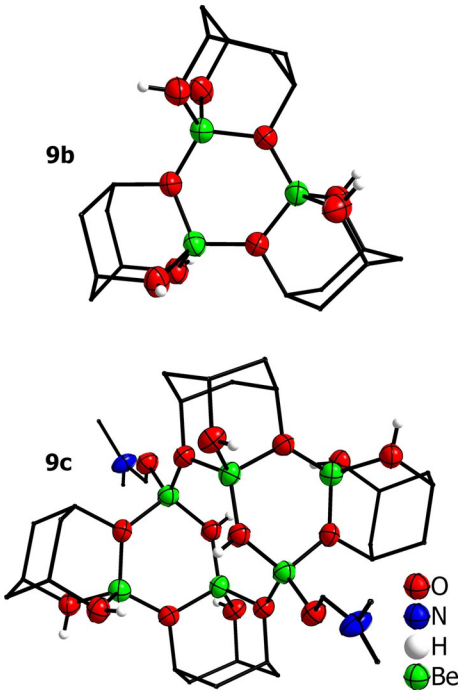

Figure 5. Molecular structures of the complex cations of **9b** and **9c**. Ellipsoids are depicted at 70% probability at 100 K. Carbon-bound hydrogen atoms are omitted and carbon atoms are shown as wire frame for clarity. Subfigures are not to scale with each other.

molecule and the μ_2-olate groups of a singly deprotonated **8** ligand, that binds κ^3 towards the third Be atom, which is not part of the eight-membered Be–O-heterocycle. It is also coordinated by the μ_2-olate group of the doubly deprotonated **8** ligand to complete the six-membered ring. The Be–O atomic distances towards the hydroxy groups range from 1.679(3) to 1.692(2) Å. These distances are significantly longer compared to the diol complexes **4a–c** and correspond best to those of the axial hydroxy groups of the cyclohexyl rings of **4a** and **4c** as expected. The Be–O atomic distances towards the μ_2-olate groups (1.554(2)–1.633(2) Å) are comparable to the corresponding distances in **2a**. The Be–O atomic distances towards the hydroxide anions (1.561(3) and 1.600(2) Å) fit into those of the olate groups as well. The O-Be-O bite angles in **9c** (100.4(1)–107.6(1)°) tend to be larger than those in the diol complexes and approach the ideal tetrahedron angle. The origin of the hydroxide anions is unclear, since we assume that all manipulations were performed under the strict exclusion of water. Furthermore, the large amount of **9c** obtained opposes introduction of H_2O through a leak of the reaction vessel. Therefore, we assume that water was generated by dehydration of **8**. Further spectroscopic investigations were constrained to IR spectroscopy as **9c** is insoluble in anhydrous solvents. As expected the O–H stretching frequency is shifted to lower wave numbers. The bathochromic shift of roughly 500 cm^{-1} is lower than those observed for the diol-complexes. Furthermore, the significant carbonyl band of the DMF ligand is visible at 1665 cm^{-1} as well as a hydroxide band at 3302 cm^{-1}. The unexpected structure of **9c** clearly shows that even unusual motifs are formed to preserve the tetrahedral coordination environment around the beryllium atom.

Compared to **9c**, **9b** shows shorter Be–O atomic distances towards the hydroxy groups (1.653(4)–1.672(4) Å) as well as shorter Be–O atomic distances towards the μ_2-olate groups (1.559(4)–1.605(4) Å). This indicates a stronger interaction between the ligands and Be^{2+}, which is plausible since there are neither DMF molecules nor hydroxide ligands present to compete. A comparison of the ligand bite angles to **9c** reveals nearly identical values of 99.1(2) to 107.8(2)°. The O-Be-O angles within the heterocycle of **9b** range from 112.0(2) to 114.5(2)°. This little deviation from 109.47° indicates a stable coordination around the Be^{2+} cation. The stability of **9c** and **9b** is further proven when both compounds are exposed to air. Single crystals of both compound were stable for hours under immersion oil, while those of **3a–c** and **2a** readily liquified within several minutes. The stability of **9b** at ambient temperature has been unexpected in the sense that it is an SO_2 solvate. However, the SO_2 molecules are heavily disordered in the crystal structure. We assume that the formation of the complexes **9b** and **9c** is the result of the deprotonation of **8** and subsequent cleavage of HCl. Although the reaction equilibrium is on the side of the starting material **9a**. Only the use of beryllium metal as a HCl scavenger shifts the equilibrium towards **9b** and **9c** that features single- and double-deprotonated **8** ligands and in the latter compound also hydroxide anions. This indicates that compounds **9c** and **9b** are basic and not stable in the rather acidic environment that is set up by the starting materials.

Although the κ^3-coordination to anionic ligands around the beryllium provides rather stable compounds, we doubt that this plays a major role in relation to monomeric sugars in the body, as these compounds are rather basic and the non-deprotonated triol **8** is not capable to compete with a large excess of methanol or H_2O. However, it seems very likely that in a polysaccharide or glycoprotein a κ^3-coordination to one saccharide segment complemented by coordination of an additional *O*-donor site, which facilitates tetrahedral coordination around the beryllium atom, is able to irreversibly bind Be^{2+} ions.

Action of beryllium ions towards sugars

To test our results regarding the reactivity of $BeCl_2$ towards the investigated model ligands for glucose and fructose, respectively, we reacted $BeCl_2$ with these two carbohydrates in non-coordinating as well as coordinating solvents. When $BeCl_2$ is mixed with glucose or fructose in non-coordinating solvents like $CDCl_3$ or CD_2Cl_2 none of the reactants dissolvs and no obvious reaction occurs at ambient temperature. When these mixtures were heated under reflux for several minutes, the starting materials turned brownish, indicating the decomposition of the sugars. To double check if this decomposition is beryllium related, glucose and fructose, respectively were heated in $CDCl_3$ as well as in CD_2Cl_2 without $BeCl_2$ and no color change was observed. In acetonitrile $BeCl_2$ dissolved while the sugars did not and within three days of storage the sugars turned

into a brownish oil. When DMF was used, the starting materials dissolve readily and the solution turn brownish within several days at ambient temperature. In contrast to that, the sugars are stable in aqueous $BeCl_2$ solution for weeks. However the ^{9}Be NMR spectra only showed the signal of $[Be(OH_2)_4]^{2+}$. As neither glucose nor fructose seemed stable in the presence of $BeCl_2$ in anhydrous solvents, we guess that a Lewis acid catalyzed dehydration reaction occurs. The reaction is well described for related Lewis acids like $AlCl_3$ or $CrCl_3$, which catalyze the formation of hydroxymethylfurfural (HMF) and its subsequent degradation to levulinic acid or humins.[22,26–29] The latter appears to be the main product in case of $BeCl_2$, since all experiments ended up in brownish suspensions. However, attempts to obtain a HMF-Be complex directly from HMF and $BeCl_2$ also failed, since the reaction solution rapidly turned into a brownish suspension as well.

To prevent the decomposition of glucose by beryllium but still obtain a possible coordination compound, α-D-methylglucoside was used instead. Since this molecule has no open chain isomer like glucose, it cannot expose an aldehyde function to $BeCl_2$. Again we were forced to use DMF to dissolve the starting materials. The solution showed no signs of decomposition for several weeks, remained clear and colorless, and the NMR spectra were similar to those of the corresponding experiment with **8**. However if the solvent is heated, decomposition occurs above approximately 50 °C (Scheme 4).

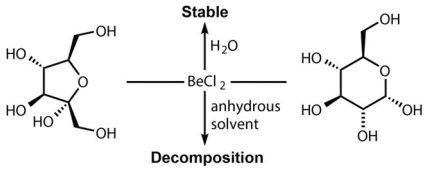

Scheme 4. Fructose and glucose decompose in anhydrous $BeCl_2$ solutions.

These results further support our assumption that monosaccharides do not play an important role for Be^{2+} coordination in the body. Furthermore, the beryllium-induced decomposition at elevated temperature suggests that upon inclusion of the Be^{2+} ion inside a glycoprotein or polysaccharide Lewis acid induced alterations of the bio-molecules can occur.

Coordination modes at beryllium related metals

To put the obtained results in relation and to evaluate to what extent the Be^{2+} ion is comparable to related metal cations like Li^+, Mg^{2+}, Al^{3+}, and Zn^{2+}, we carried out a set of experiments with these and the *cis*-1,2-diols **1a** and **1b**. For this purpose, two equivalents **1a** or **1b** were reacted with one equivalent metal chloride in $CDCl_3$. The resulting reaction solutions differed not only in relation to those obtained for $BeCl_2$ but also in relation to each other. For LiCl and $ZnCl_2$ we obtained nearly no precipitates while $MgCl_2$ yields a voluminous precipitate. In case of $AlCl_3$, the solutions solidified into a gel, which was subsequently filtered by means of a specially designed adapter from one J. Young NMR tube into another, which is illustrated in Figure S2, Supporting Information. The filtered Al^{3+}-solutions showed signals of free ligand in the case of **1a** with nearly no intensity while for the solution of **1b** no signals were observed in the NMR spectra. The separated precipitates were amorphous which was determined by powder X-ray diffraction. For the other metal chlorides the NMR experiments were performed without prior filtration. The received ^{1}H and ^{13}C NMR spectra are shown in Figures S41–S44, Supporting Information. In the ^{1}H NMR spectra, we observe a much smaller impact on the protons due to coordination to the metal chlorides compared to $BeCl_2$ (see also the Supporting Information, Table S6). The largest downfield shifts were observed for $MgCl_2$ while $ZnCl_2$ showed almost no influence on the diols. The NMR spectra of the solutions containing beryllium related metal chlorides also showed basically no line broadening compared to the corresponding solutions of $BeCl_2$. Additionally, we did not observe any influence on the diol carbon nuclei in the ^{13}C NMR spectra, when beryllium related metal chlorides were present.

To get a better understanding of the influence of LiCl, $MgCl_2$, $AlCl_3$, and $ZnCl_2$ on the hydroxy groups of the tested diols **1a** and **1b** compared to $BeCl_2$, the solvent was removed in vacuo from the reaction solutions and the obtained solids were analyzed by IR spectroscopy. For Al^{3+} we used the prior separated precipitates. The obtained IR spectra are illustrated in Figures S64 and S65, Supporting Information. The results correlate well with the chemical shifts observed in the ^{1}H NMR spectra. While LiCl and $ZnCl_2$ have little influence on the hydroxy groups, $MgCl_2$ induces a noticeable bathochromic shift of the O–H stretching frequency, while the bathochromic shift of this band in the Al^{3+}-containing compound even exceeds that of the corresponding Be^{2+} compound by nearly 100 cm^{-1}. It shows also stronger line broadening compared to the corresponding spectrum with $BeCl_2$, indicating the formation of some kind of coordination polymer, which correlates with the observed formation of gels. Quintessentially Zn^{2+} and Li^+ show the least similarity to Be^{2+}, whereas Al^{3+} is the most comparable to Be^{2+} among the tested metal cations. This is expected due to the similar charge to ion radius ratio of the latter two metal ions as described by their diagonal relationship in the periodic table. However these findings enable only comparison of the relative charge to radius ratio of the ions and do not take into account that the coordination sphere around the metal cations may differ, which is a tremendous factor when it comes to complexation inside an active site of an enzyme or other large biomolecules. Therefore, attempts have been made to obtain single-crystal structures of all tested metal chlorides under similar conditions to compare their preferred coordination environments.

In case of LiCl, the previously studied reaction solution of **1b** yielded single crystals of bis(κ^2-*cis*-1-μ_2-hydroxy-2-hydroxycyclopentanediol)bis(κ^2-*cis*-1,2-cyclopentanediol)dilithium dichloride·*cis*-1,2-cyclopentanediol (**10a**) after two weeks of storage at ambient temperature. Compound **10a** crystallizes as colorless columns in the triclinic space group $P\bar{1}$. Its formation is illustrated in Scheme 5.

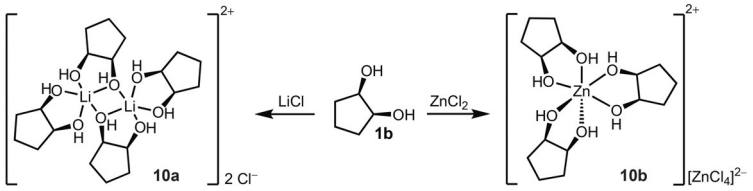

Scheme 5. Reaction of **1b** with LiCl and $ZnCl_2$ in $CDCl_3$ to yield **10a** and **10b**, respectively.

Compound **10a** features two Li atoms that are μ_2-bridged by two hydroxy groups of two **1b** ligands to form a four-membered Li–O ring (Figure 6). The bridging diols bind κ^2 to one lithium atoms each and another **1b** binds to each Li atom to complete the distorted trigonal bipyramidal coordination sphere around the lithium atoms. The same structure motive is reported for germanium as central atoms.[45] However, in the case of Ge^{4+} the diol ligands are fully deprotonated, whereas in **10a** none of the hydroxy groups are deprotonated. The Li–O atomic distances to the terminal diol are 1.946(3) and 2.016(3) Å and those within the fourfold heterocycle are 2.074(3) and 2.169(3) Å, which is significantly larger. These values are, therefore, much larger than those found in **2a** and **3b**. Consequently, the O-Li-O bite angles are significantly smaller than those in **2a** and **3b**.

In case of $ZnCl_2$ the prior obtained precipitates were recrystallized from $CDCl_3$ at ambient temperature within a few days to yield block-shaped crystals of tris(κ^2-*cis*-1,2-cyclopentanediol)zinc tetrachloridozincate (**10b**, Figure 6, Scheme 5) in the monoclinic space group $P2_1/n$. Here the $ZnCl_2$ selfionizes into a $[ZnCl_4]^{2-}$ anion and a Zn^{2+} cation that is octahedrally coordinated by the hydroxy groups of three **1b** ligands. The Zn–O atomic distances in **10b** range from 2.058(2) to 2.117(2) Å, which are similar to those in **10a**. Also the O-Zn-O bite angles of 76.4(1)–77.8(1)° match those of **10a**. The $[Zn(\mathbf{1b})_3]^{2+}$ cations are interconnected by the zincate anions through hydrogen bonds.

While we were able to obtain single crystals of **10a** and **10b** in a non-coordinating solvent, we had to use coordinating solvents to recrystallize the precipitates obtained for $MgCl_2$ and $AlCl_3$, which is indicative for the presence of coordination polymers or highly charged species. Unlike for $BeCl_2$ and $BeBr_2$, respectively, the use of SO_2 did not work. For the magnesium compound the use of DMF was necessary to obtain several millimeter long plate-shaped crystals of bis(κ^2-*cis*-1,2-cyclopentanediol)bis(dimethylformamide)magnesium dichloride (**10c**, Figure 6, Scheme 6), which crystallizes in the

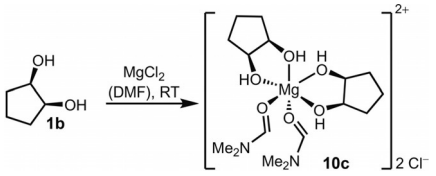

Scheme 6. Reaction of **1b** with $MgCl_2$ in DMF to yield **10c**.

monoclinic space group $P2_1/n$. Unlike the other cationic species obtained with **1b**, compound **10c** is coordinated by ligands other than **1b**. In **10c** the Mg atom is octahedrally coordinated by four oxygen atoms of two **1b** and two dimethylformamide molecules. In comparison to **10b** compound **10c** does not only show a similar octahedral coordination but also equal O_{diol}-metal-O_{diol} bite angles (76.(1) and 77.1(2)°). The Mg–O atomic distances to the diols are also nearly identical to the corresponding distances in **10b** (2.029(8)–2.093(1) Å). The O-Mg-O angle between the two DMF molecules is 90.5(1)°, which

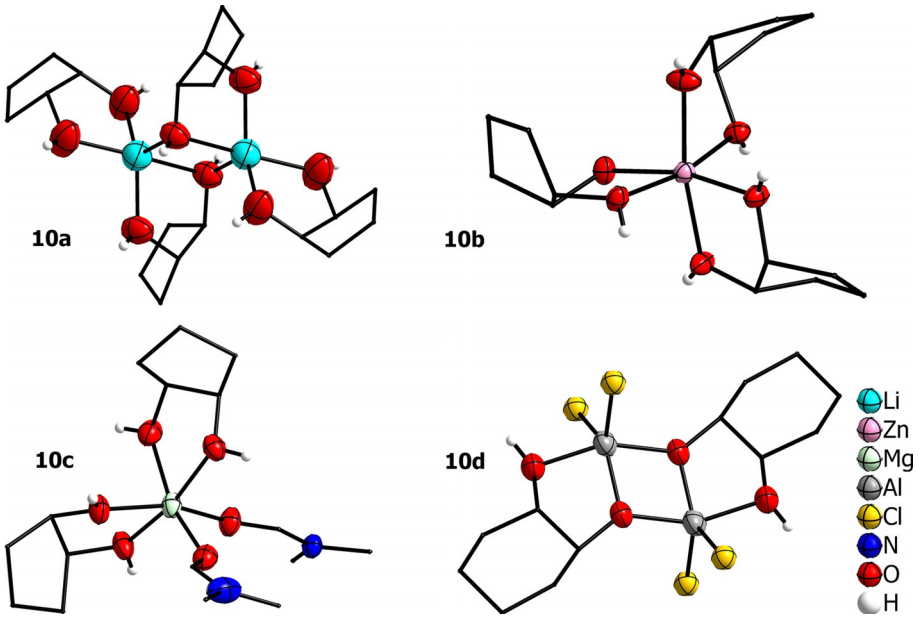

Figure 6. Molecular structures of the cations in compounds **10a–c** and of complex **10d**. Ellipsoids are depicted at 70% probability at 100 K. Carbon-bound hydrogen atoms are omitted and carbon atoms are shown as wire frame for clarity. Subfigures are not to scale with each other.

is larger than the bite angles of the diols. This may explain why the coordination through a third diol is not favored over the DMF molecules, since the smaller bite angle would put more strain into the octahedral coordination environment around the Mg^{2+} cation.

In case of $AlCl_3$ we were not able to obtain crystalline compounds with **1b** in a variety of solvents and we always ended up with amorphous solids. The use of **1a** as the ligand in THF as the coordinating solvent yielded needle-shaped single crystals of bis(κ^2-*cis*-1-μ_2-olate-2-hydroxy-cyclopentane)dialuminium tetrachloride·2THF (**10d**, Figure 6, Scheme 7), which crystallizes in the monoclinic space group *P*21/*c*. Compound **10d** features two Al^{3+} cations that are linked through two deprotonated hydroxy groups of **1a** to form a fourfold Al–O heterocycle comparable to that of **10a**. The second hydroxy group of the two coordinating diols remains protonated. In contrast to the other beryllium related metal chlorides, $AlCl_3$ does not form a cationic species under the dissociation of Cl ions, but two Cl atoms remain bound to each Al atom to complete the distorted trigonal bipyramidal coordination sphere around it. The cleavage of HCl during the formation of **10d** is similar to **2a** and is evidence for the similar charge to radius ratio of the two metal ions. The Al–O atomic distance to the hydroxy group is 1.938(3) Å, while the corresponding distance to the deprotonated OH group is 1.835(3) Å, which are both significantly longer than the corresponding distances in the beryllium compounds. The O-Al-O bite angles (81.0(1)°) are also not comparable with those of **3** or **2a** and behave more like those of the other metal chlorides. However, the comparison between **10d** and related dinuclear bis(κ^2-1-μ_2-olate-2-hydroxy-3-methylcyclohexane)dialuminium tetrachloride shows great similarity,[46] since not only the atomic distances are similar, but also the coordination of the crystal THF molecules are identical, that bind through hydrogen bonding to the hydroxy groups. Although $AlCl_3$ is the most comparable metal halide to $BeCl_2$, it was not possible to obtain analogous compounds to those obtained for $BeCl_2$.

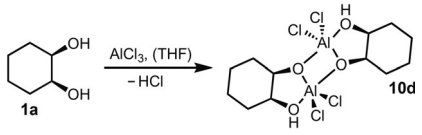

Scheme 7. Reaction of **1a** with $AlCl_3$ in THF to yield **10d**.

To put it in a nutshell, it is not possible to mimic the coordination environment around the Be^{2+} cation with the tested metal chlorides under the employed conditions. We, therefore, assume that it is not feasible to substitute beryllium with related metals when bonding modes are investigated in restrained coordination environments, like in active sites or large chelate ligands.

Conclusions

It has been shown that glucose and fructose are decomposed by $BeCl_2$ under anhydrous conditions into various humins. Through the use of α-D-methylglucoside we were able to limit the cause of the degradation to the aldehyde/hemiacetal function. However, no corresponding complex could be obtained with beryllium, to determine a possible coordination within a carbohydrate. To mimic possible binding sites, various cyclic diols **1**, triol **8** as well as furanyl **5c** and pyranyl **5b** alcohols were reacted with $BeCl_2$. Thereby single crystals of diol complexes **3a**–**c** and **2a** as well as of compounds **2b**, **9b**, and **9c** were isolated. Competition experiments revealed a distinct trend in the relative binding affinity towards beryllium among the tested ligands, leaving tridentate **8** as the most potent ligand followed by *cis*-1,3-diols, while the *trans*-diols seem to form no stable complexes. This trend is compiled in Scheme 8. From reactions in water it is obvious that neither κ^2- nor κ^3-chelation is sufficient to compete against a huge excess of H_2O molecules. Therefore, it is unlikely that monosaccharides in solution play a role in beryllium ion binding in the body. However in view of the large increase in complex stability from κ^2- to κ^3-coordination it seems very likely that in a polysaccharide or glycoprotein a κ^3-coordination to one saccharide segment complemented by coordination of an additional *O*-donor site can facilitate irreversible Be^{2+} ion binding. This additional ligation site is very likely a hydroxy group or a carboxylate[35] since these proved to be distinctly superior to oxygen atoms of glycosidic bonds.

Complexes **9b** and **9c** with deprotonated triol **8** are formed only when this ligand is reacted with $BeCl_2$ and Be at forcing conditions. Together with compounds **2a** and **2b** these multinuclear complexes reveal the frequent formation of Be–O heterocycles. Even though the beryllium ion concentration in the body is expected to be low, it should not be excluded that the actual cause of beryllium associated diseases is the formation of polynuclear Be-complexes inside proteins and glycans, considering the long latency times. It should be mentioned that the $[Be_4O]^{6+}$ core has already been suggested as a potential key agent in chronic beryllium disease.[47]

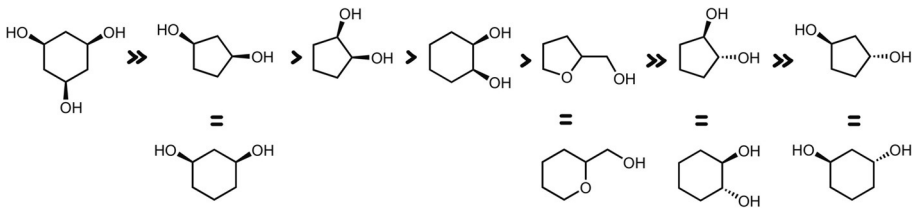

Scheme 8. Relative binding affinities of the tested chelating alcohols towards Be^{2+}.

Neither in solution nor in the solid state was Be^{2+} non-tetrahedrally surrounded. Therefore, we are confident that Be^{2+} cations are exclusively coordinated in a tetrahedral environment in vivo and this should be taken into account in the search for potential beryllium binding sites and in the development of beryllium selective ligands.

Furthermore, the formation of **2a**, **2b**, **9b**, and **9c** through HCl cleavage in the absence of base, demonstrates that beryllium coordinated chelating alcohols can act as potent Brønstedt acids. This, in addition with the observed Lewis acid related decomposition of monosaccharides also suggests that, upon inclusion into glycoproteins or polysaccharides, beryllium ions can induce alterations of these biomolecules.

When Li^{+}, Mg^{2+}, Al^{3+}, and Zn^{2+} were reacted with **1b** and **1a** none of them showed the same coordination behavior towards the diols compared to Be^{2+} and only Al^{3+} matched the reactivity and charge to ion radius ratio of Be^{2+}. Moreover, a tetrahedral coordination around these metal ions was never achieved as evident from compounds **10a**–**d**. This is an important aspect for a potential substitution of beryllium in in vivo experiments, since the above mentioned metal ions, which best match the ratio of ion radius and charge of Be^{2+}, are not suitable for this purpose. Consequently, to understand how beryllium affects macromolecules, it cannot be substituted by other metals.

Experimental Section

General

The Supporting Information contains detailed experimental procedures, analytical data, tables with crystallographic details, and NMR and IR coordination shifts as well as selected NMR and IR spectra. CCDC 1939419, 1939420, 1939421, 1939422, 1939423, 1939424, 1939425, 1939426, 1939427, 1939428, and 1939429 contain the supplementary crystallographic data for this paper. These data are provided free of charge by The Cambridge Crystallographic Data Centre.

Acknowledgements

M.R.B. thanks Prof. F. Kraus for moral and financial support as wells as the provision of laboratory space. The DFG is gratefully acknowledged for financial support (BU2725/5-1 & BU2725/8-1).

Conflict of interest

The authors declare no conflict of interest.

Keywords: beryllium · carbohydrates · coordination chemistry · diols · main-group chemistry

[1] M. Leslie, *Science* **2013**, *341*, 26 – 27.
[2] S. C. Eisenbarth, O. R. Colegio, W. O'Connor, F. S. Sutterwala, R. A. Flavell, *Nature* **2008**, *453*, 1122 – 1126.
[3] S. Hutchison, R. A. Benson, V. B. Gibson, A. H. Pollock, P. Garside, J. M. Brewer, *FASEB J.* **2012**, *26*, 1272 – 1279.
[4] A. L. Gavin, K. Hoebe, B. Duong, T. Ota, C. Martin, B. Beutler, D. Nemazee, *Science* **2006**, *314*, 1936 – 1938.
[5] T. R. Ghimire, R. A. Benson, P. Garside, J. M. Brewer, *Immunol. Lett.* **2012**, *147*, 55 – 62.
[6] T. L. Flach, G. Ng, A. Hari, M. D. Desrosiers, P. Zhang, S. M. Ward, M. E. Seamone, A. Vilaysane, A. D. Mucsi, Y. Fong, E. Prenner, C. C. Ling, J. Tschopp, D. A. Muruve, M. W. Amrein, Y. Shi, *Nat. Med.* **2011**, *17*, 479 – 487.
[7] A. S. McKee, M. A. Burchill, M. W. Munks, L. Jin, J. W. Kappler, R. S. Friedman, J. Jacobelli, P. Marrack, *Proc. Natl. Acad. Sci. USA* **2013**, *110*, E1122 – E1131.
[8] L. S. Newman, *Science* **1993**, *262*, 197 – 198.
[9] A. P. Fontenot, T. S. Keizer, M. McCleskey, D. G. Mack, R. Meza-Romero, J. Huan, D. M. Edwards, Y. K. Chou, A. A. Vandenbark, B. Scott, G. G. Burrows, *J. Immunol.* **2006**, *177*, 3874 – 3883.
[10] G. M. Clayton, Y. Wang, F. Crawford, A. Novikov, B. T. Wimberly, J. S. Kieft, M. T. Falta, N. A. Bowerman, P. Marrack, A. P. Fontenot, S. Dai, J. W. Kappler, *Cell* **2014**, *158*, 132 – 142.
[11] F. R. Dutra, *Am. J. Pathol.* **1948**, *24*, 1137 – 1165.
[12] J. D. Stoeckle, H. L. Hardy, A. L. Weber, *Am. J. Med.* **1969**, *46*, 545 – 561.
[13] D. Kriebel, J. D. Brain, N. L. Sprince, H. Kazemi, *Am. Rev. Respir. Dis.* **1988**, *137*, 464 – 473.
[14] D. N. Skilleter, *Chem. Ber.* **1990**, *26*, 26 – 30.
[15] M. J. Allen, A. Laederach, P. J. Reilly, R. J. Mason, *Biochemistry* **2001**, *40*, 7789 – 7798.
[16] P. M. Rudd, M. R. Wormald, R. L. Stanfield, M. Huang, N. Mattsson, J. A. Speir, J. A. DiGennaro, J. S. Fetrow, R. A. Dwek, I. A. Wilson, *J. Mol. Biol.* **1999**, *293*, 351 – 366.
[17] B. S. Bochner, N. Zimmermann, *J. Allergy Clin. Immunol.* **2015**, *135*, 598 – 608.
[18] A. K. Shrive, H. A. Tharia, P. Strong, U. Kishore, I. Burns, P. J. Rizkallah, K. B. Reid, T. J. Greenhough, *J. Mol. Biol.* **2003**, *331*, 509 – 523.
[19] H. Sahly, Y. Keisari, E. Crouch, N. Sharon, I. Ofek, *Infect. Immun.* **2008**, *76*, 1322.
[20] H. Xiao, E. C. Woods, P. Vukojicic, C. R. Bertozzi, *Proc. Natl. Acad. Sci. USA* **2016**, *113*, 10304 – 10309.
[21] D. Naglav, M. R. Buchner, G. Bendt, F. Kraus, S. Schulz, *Angew. Chem. Int. Ed.* **2016**, *55*, 10562 – 10576; *Angew. Chem.* **2016**, *128*, 10718 – 10733.
[22] Y. Zhang, E. A. Pidko, E. J. M. Hensen, *Chem. Eur. J.* **2011**, *17*, 5281 – 5288.
[23] X. Zhang, P. Murria, Y. Jiang, W. Xiao, I. Kenttamaa, Hilkka, M. M. Abu-Omar, N. S. Mosier, *Green Chem.* **2016**, *18*, 5219 – 5229.
[24] L. Peng, L. Lin, J. Zhang, J. Zhuang, B. Zhang, Y. Gong, *Molecules* **2010**, *15*, 5258 – 5272.
[25] V. Choudhary, S. H. Mushrif, C. Ho, A. Anderko, V. Nikolakis, N. S. Marinkovic, A. I. Frenkel, S. I. Sandler, D. G. Vlachos, *J. Am. Chem. Soc.* **2013**, *135*, 3997 – 4006.
[26] H. Zhao, J. E. Holladay, H. Brown, Z. C. Zhang, *Science* **2007**, *316*, 1597 – 1600.
[27] X. Li, K. Peng, X. Liu, Q. Xia, Y. Wang, *ChemCatChem* **2017**, *9*, 2739 – 2746.
[28] Y. Román-Leshkov, M. Moliner, J. A. Labinger, M. E. Davis, *Angew. Chem. Int. Ed.* **2010**, *49*, 8954 – 8957; *Angew. Chem.* **2010**, *122*, 9138 – 9141.
[29] H. Nguyen, V. Nikolakis, D. G. Vlachos, *ACS Catal.* **2016**, *6*, 1497 – 1504.
[30] R. Noma, K. Nakajima, K. Makata, M. Kitano, S. Hayashi, M. Hara, *J. Phys. Chem. C* **2015**, *119*, 17117 – 17125.
[31] M. R. Buchner, *Chem. Eur. J.* **2019**, *25*, 12019 – 12036.
[32] N. A. Bell, G. E. Coates, H. M. M. Shearer, J. Twiss, *J. Chem. Soc. Chem. Commun.* **1983**, 840 – 841.
[33] J. Gottfriedsen, S. Blaurock, *Z. Anorg. Allg. Chem.* **2005**, *631*, 3037 – 3039.
[34] P. Klüfers, P. Mayer, J. Schuhmacher, *Z. Anorg. Allg. Chem.* **1995**, *621*, 1373 – 1379.
[35] M. Müller, M. R. Buchner, *Angew. Chem. Int. Ed.* **2018**, *57*, 9180 – 9184; *Angew. Chem.* **2018**, *130*, 9321 – 9325.
[36] P. G. Plieger, K. D. John, T. S. Keizer, T. M. McCleskey, A. K. Burrell, R. L. Martin, *J. Am. Chem. Soc.* **2004**, *126*, 14651 – 14658.
[37] A. Kumar, G. S. McGrady, J. Passmore, F. Grein, A. Decken, *Z. Anorg. Allg. Chem.* **2012**, *638*, 744 – 753.
[38] D. Shopova, R. Dinnebier, M. Jansen, *Z. Naturforsch. Sect. B* **2008**, *63*, 1087 – 1092.
[39] P. Delangle, C. Husson, C. Lebrun, J. Pécaut, P. J. A. Vottéro, *Inorg. Chem.* **2001**, *40*, 2953 – 2962.

[40] O. Kumberger, J. Riede, H. Schmidbaur, *Chem. Ber.* **1992**, *125*, 2701 – 2703.
[41] L. Hiltunen, L. Markku, N. Lauri, S. Reijo, *Acta Chem. Scand. Sect. A* **1983**, *38*, 201 – 209.
[42] R. Sillanpää, T. Nortia, L. Hiltunen, *Inorg. Chim. Acta* **1984**, *83*, 111 – 114.
[43] M. Müller, M. R. Buchner, *Chem. Eur. J.* **2019**, *25*, 11147 – 11156.
[44] M. R. Buchner, M. Müller, F. Dankert, K. Reuter, C. von Hänisch, *Dalton Trans.* **2018**, *47*, 16393 – 16397.
[45] P. Klüfers, C. Vogler, *Z. Anorg. Allg. Chem.* **2007**, *633*, 908 – 912.
[46] F. Bélanger-Gariépy, K. Hoogsteen, V. Sharma, J. D. Wuest, *Inorg. Chem.* **1991**, *30*, 4140 – 4145.
[47] R. J. F. Berger, R. Mera-Adasme, *Z. Naturforsch. Sect. B* **2016**, *71*, 71 – 75.

Manuscript received: July 29, 2019
Revised manuscript received: September 5, 2019
Accepted manuscript online: September 9, 2019
Version of record online: November 8, 2019

